Ordered Silicon Pillar Arrays Prepared by Electrochemical Micromachining: Substrates for High Efficiency Cell Transfection

Frances J. Harding,[†] Salvatore Surdo,[‡] Bahman Delalat,[†] Chiara Cozzi,[‡] Roey Elnathan,[†] Stan Gronthos,[§] Nicolas H. Voelcker[†] and Giuseppe Barillaro*[‡]*

† ARC Centre of Excellence in Convergent Bio-Nano Science and Technology, Future Industries Institute, Mawson Lakes, University of South Australia 5095, Australia.

‡ Dipartimento di Ingegneria dell'Informazione, Università di Pisa, via G. Caruso 16, 56122 Pisa, Italy.

§ South Australian Health and Medical Research Institute, Adelaide 5000, South Australia, Australia, Australia. Mesenchymal Stem Cell Group Laboratory, School of Medicine, Faculty of Health Sciences, University of Adelaide, Adelaide, South Australia, Australia.

KEYWORDS: silicon nanostructures, pillars, transfection, topography, cell alignment.

ABSTRACT: Ordered arrays of silicon nano- to microscale pillars are used to enable biomolecular trafficking into primary human cells, consistently demonstrating high transfection efficiency can be achieved with broader and taller pillars that reported to date. Cell morphology

on the pillar arrays is often strikingly elongated. Investigation of the cellular interaction with the pillar reveals that cells are suspended on pillar tips and do not interact with the substrate between the pillars. While cells remain suspended on pillar tips, acute local deformation of the cell membrane was noted, allowing pillar tips to penetrate the cell interior, while retaining cell viability.

As the scale of material features approach that of cells and then decrease further, increased interaction at the interface between cells and materials becomes possible. Three dimensional arrays can be constructed to topographically resemble a bed of nails scaled-down to the nano-scale. Cell interaction with these surface topographies permeabilizes cell membranes without compromising cell viability, presenting a means to traffic biomolecules, including DNA and other genetic material, into the cell interior.[1-5] This enhanced molecular trafficking, whilst a complex process, has been attributed to the penetration of lipid bilayer by the nanostructure, allowing direct access to the cell cytoplasm and bypassing the vagaries of endocytotic uptake.[6] This is termed "impalefection". Complete penetration of the nanostructures into the cell interior has been reported to be a rare event, but its frequency can be increased by manipulating cell-surface interaction, for example by tuning surface chemistry.[6-9] As a result, molecular DNA uptake reported in some cases has been astoundingly high, reaching 95% of the cell population, with a concordantly high level of transfection efficiency.[1,5] Impalefection can avoid the immunogenicity and toxicity issues that hinder other viral and non-viral transfection.[2,3] The innovation of this approach has been demonstrated in high throughput siRNA knockdown screens to delineate complex transcriptional networks.[10]

Typically, nanostructure arrays that have been used to traffic biomolecules into cells have been non-ordered, with randomly placed features.[2] Precisely aligned uniform arrays convey an advantage when investigating pillar mediated transfection, reducing variability between the microenvironment each cell is exposed to and eliciting a more homogenous response.[3,5] The efficiency of transfection reported from various sources on vertical nanostructure arrays is notably discordant.[2,3] Geometrical parameters that define a nanostructured surface – the diameter and length of features and spacing between – are known to impact the achievement of cell penetration and subsequently transfection.[5,11] Small changes in these physical parameters can result in a conspicuous change in cell response to array topography.[12-14] Cell adhesion to the underlying substrate has been identified as the predominant mechanism governing nanowire penetration into cells, since forces generated though adhesion are large enough to induce local membrane rupture.[7,15]

Here we present a method of pillar array construction by electrochemical micromachining that produces precisely aligned pillars of high aspect ratio (>10) and dimension and spacing tunable to a large extent by manipulating parameters in the fabrication process. In this work we focus on arrays of regular pillars with diameters of 500 to 1000 nm and spacing of 8 μm. We examine the capacity of these manufactured arrays to transfect primary cells, demonstrating consistently that high transfection efficiency can be achieved with pillars broader and taller than those reported previously.

Fabrication of out-of-plane silicon pillars was carried out by electrochemical micromachining[16-18] as shown in Figure 1. The starting material used was n-type silicon, of orientation (100), with a thin silicon dioxide layer on top. Two lithographical patterning methods were considered to produce pillar arrays: an array of square patches with size of 4 μm and spatial period of 8 μm

(type 1 pillars, Figure 1A) or square holes with size of 6 μm and spatial period of 8 μm (type 2 pillars, Figure 1C) were defined on a photoresist layer by standard lithography and transferred to the silicon dioxide layer by buffered HF (BHF) etching through the photoresist mask, replicated (seed-point formation) into the silicon surface by potassium hydroxide (KOH) etching through the silicon dioxide mask, and finally anisotropically etched into the bulk material to a depth of 10 μm by back-side illumination electrochemical etching (BIEE). A thermal oxidation step was carried out to partially convert silicon to silicon-dioxide so as to grow a 1-μm-thick conformal silicon-dioxide layer encapsulating a two-dimensional array of out-of-plane silicon pillars. An HF-based etching step was subsequently performed to remove the silicon dioxide layer and reveal the array of silicon pillars, which have a period of 8 μm, a height of 10 μm, and an average diameter of 1000 ± 100 nm (Figure 1A) and 500 ± 50 nm (Figure 1C) .

Scanning electron microscope (SEM) bird-eye-view images (at different magnifications) of out-of-plane pillars fabricated by the above described process using the two lithographical patterning are shown in Figure 1B and Figure 1D, which highlight that high reliability in fabrication and good uniformity in pillar size can be achieved for both patterning approaches. We observed changes in the apical surfaces of the wires produced with the two techniques: a more rounded "match-stick" process characterized type 1 pillars, whereas type 2 pillars were flat topped, but possessed sharp edges at the top formed by the square cross section. The approach outlined in Figure 1C has certain advantages over the approach in Figure 1A in terms of reproducibility and uniformity of the pillar morphology, across the same chip and from chip to chip, but both approaches nevertheless afford high quality arrays of pillars. By manipulating fabrication parameters both height and spacing of pillars can be tuned to a large extent (Figure S1).

Next, the capacity of the pillar substrates for cell transfection was assessed. Prior to cell transfection studies, pillar arrays were coated with poly-D-lysine (PDL) and then plasmid DNA encoding green fluorescent protein (GFP). Amine functionalization provided by PDL coating serves a two-fold purpose: to bind plasmid DNA and to promote the impalefection of cells by initiating and maintaining intracellular access.[5,8] Using human foreskin fibroblasts (HFF), similar levels of cell transfection, measured by green fluorescence intensity of the cell population, were observed on both types of arrays constructs (Figure 2A-C) averaging 75% after 72 h, compared to very low levels of transfection on flat silicon surfaces. Control culture of HFF cells on micro pillars without plasmid coating for the same period of time did not elicit a green fluorescent signal, verifying that green fluorescence was indicative of translation of the GFP encoded in by transfected plasmid (Figure S2). Cell viability on arrays at this time (72 h after plating on DNA-coated pillars) was comparable to controls (arrays: 92.2%, control 93.7% χ^2 test p=0.44, Figure S-3). Although cell viability has been reported to be compromised on nanowires of diameter >400nm,[5] there are instances where silicon pillars of greater diameter than 400nm have been successfully employed for cell propagation.[19,20]

After 3 days culture on both type 1 and type 2 pillar arrays, a striking morphology change was observed in HFF. Elongation of cell body was particularly notable for HFF (Figure 2A, B). Filopodia extending several microns to bridge between pillars were also seen (Figure 2B, Figure 2D insets). The ordered pillar format appeared to provide a topographical cue for cell extension, with filopodia (and the cell body more generally) guided across rows or columns of pillars (Figure 2D, E). The interfacing of cells to high aspect ratio nanostructures is well documented to induce changes in cell morphology, adhesion, migration, and function.[2,3] For example, filopodia are frequently observed in greater numbers on nanostructured surfaces when compared to flat

surfaces, anchoring the cell firmly to the pillar substrate.[21-23] The elongated morphology observed here is in apparent contrast with the reduction in cytoplasmic area reported elsewhere for cells cultured on silicon nanowire substrates.[22,24] However, the previous work employed wires of smaller diameter, which were able to be bent inwards by traction forces exerted by the cell.[25,27] By bending the nanowires back towards the main cell body,[21,25,26] the contracting cell also increases the pitch between wire tips, making it more difficult for filopodia to bridge the gap to the next wire tip and spread to the adjacent tips.[21] Here, pillars remained upright within the array under cell culture conditions, stabilizing the extended cell body. A similar morphology, exhibiting elongated and aligned axon-like processes, has been previously observed to arise where nanowires are spaced at a distance that approaches the limit of filopodia to bridge.[14] pillars of both type 1 and type 2 were visible against the apical face of HFF cells (Figure 2D, E and insets), suggesting embedding of the pillars into the cell body. Multiple pillars were noted to interact with each cell (Figure 2D insets).

Various modes of cell response to vertically aligned silicon nanowires have been identified, from minimal interaction to through indentation of the cell membrane.[25] Accordingly, we investigated the cellular interaction with the pillar arrays in more depth using focused ion beam (FIB) scanning electron microscopy (Figure 3).

HFF cells were found to be suspended on the tips of pillars and did not interact with the substrate between the wires, as assumed by models of nanowire mediated transfection.[6] Close conformation of the cell body to the pillar form was observed (Figure 3A), but the pillars did not pierce the apical plasma membrane, remaining encapsulated within the cell body. However, dissection *via* the focused ion beam revealed the peripheral cell body to be stretched very thin. Perturbation of the basal plasma membrane by the pillar tip was observed in some instances

(Figure 3A). Engulfment of pillar tips was also noted in spatially isolated cells where cell morphology was more compact. In these cases, too, there was no interaction with the cell and the substrate base (Figure 3B and S-4). The precise mechanisms that regulate nanostructure mediated transfection remain controversial. The normal force generated during gravity driven settling is insufficient to impale vertically aligned nanowires through the cell membrane, other than where the nanowire geometries employed are thin, tall and arranged at low density.[1,6] The greater normal forces generated as cells adhere to the substrate at the nanowire base are more likely to rupture the plasma membrane. It is not understood whether rupture of the plasma membrane is absolutely required for nanotopography mediated transfection[6,15] or if acute cell membrane curvature may induce cell membrane porosity sufficient for molecular trafficking.[4,27,28] In a number of instances, membrane wrapping around nanowires, excluding direct access to the cytosol and nucleus have been observed.[8,29] As noted above, previous work employing nanowires for transfection have employed nanostructure diameters in the range of 100-400 nm, smaller than the pillars described here.[2,3,5] However, recent modelling would suggest that increased diameter would be conducive to membrane deformation of cells settled on tall micro pillars,[29] which is predicted to enhance endocytosis.[30]

Critical parameters of pillar topography - density, spacing (or pitch), length and diameter – inform cell response to the pillar array and require optimisation for each application in order to target specific modes of interaction.[2,5,10,29] In order to determine if the transfection results achieved with HFF were generalisable to other cell types, we attempted transfection of human primary dental pulp stem cells (DPSC, a mesenchymal stem cell population) using pillar substrates (Figure 4). Elongation of DPSC morphology was also observed on pillar substrates, together with consistently high levels of transfection (75.3 ± 12.9%). Surface chemistry was

critical for DPSC attachment to the pillar arrays. Little cell adhesion and spreading were seen in the absence of the PDL coating (Figure S-5).

Using ordered arrays of silicon pillars as a means of biomolecule trafficking, we have demonstrated that high transfection efficiency of human primary cells can be achieved with broader and taller pillars that reported to date. Cell morphology on the pillar arrays is often strikingly elongated. While cells remain suspended on pillar tips, acute local deformation of the cell membrane was noted, and on occasion, pillar tips penetrated the cell membrane. The fabrication method employed allows the modification of pillar shape as well as length and pitch, thus providing a general platform for cell transfection with morphological features complementary to those of platforms of more common use.

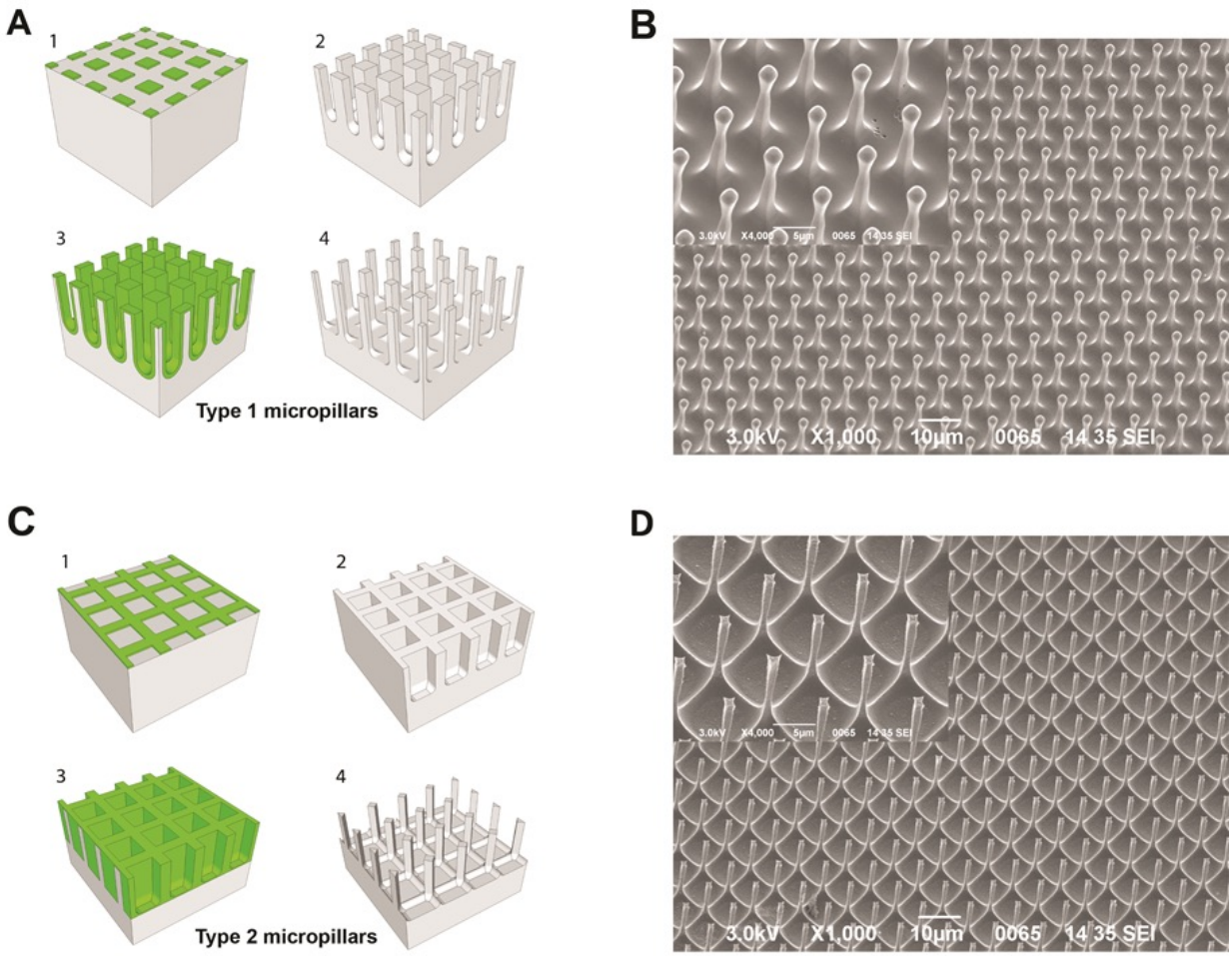

Figure 1. Pillar array fabrication: A) Through standard lithography and consecutive etching with hydrofluoric acid (HF) and KOH, a positive silicon dioxide mask (green) was defined on the silicon surface (1). The periodic square pattern was then etched into the bulk material by BIEE (2). Thermal oxidation created a silicon-dioxide layer on the pillar surface (3), allowing the diameter of the pillars to be reduced to 1000 nm through HF etching. B) Tilt SEM view of pillars produced using method described in panel A (type 1 pillars) at x1000 and 4000x magnification (inset). C) Alternative protocol for the production of ordered pillar arrays. A lattice pattern is defined on silicon surface and etched into a 3D structure as described in panel A) (1, 2). Thermal oxidation of this structure followed by HF etching produces pillars of 500 nm in diameter (3,4).

D). Tilt SEM view of pillars produced using method described in panel C (type 2 pillars) at x1000 and 4000x magnification (inset).

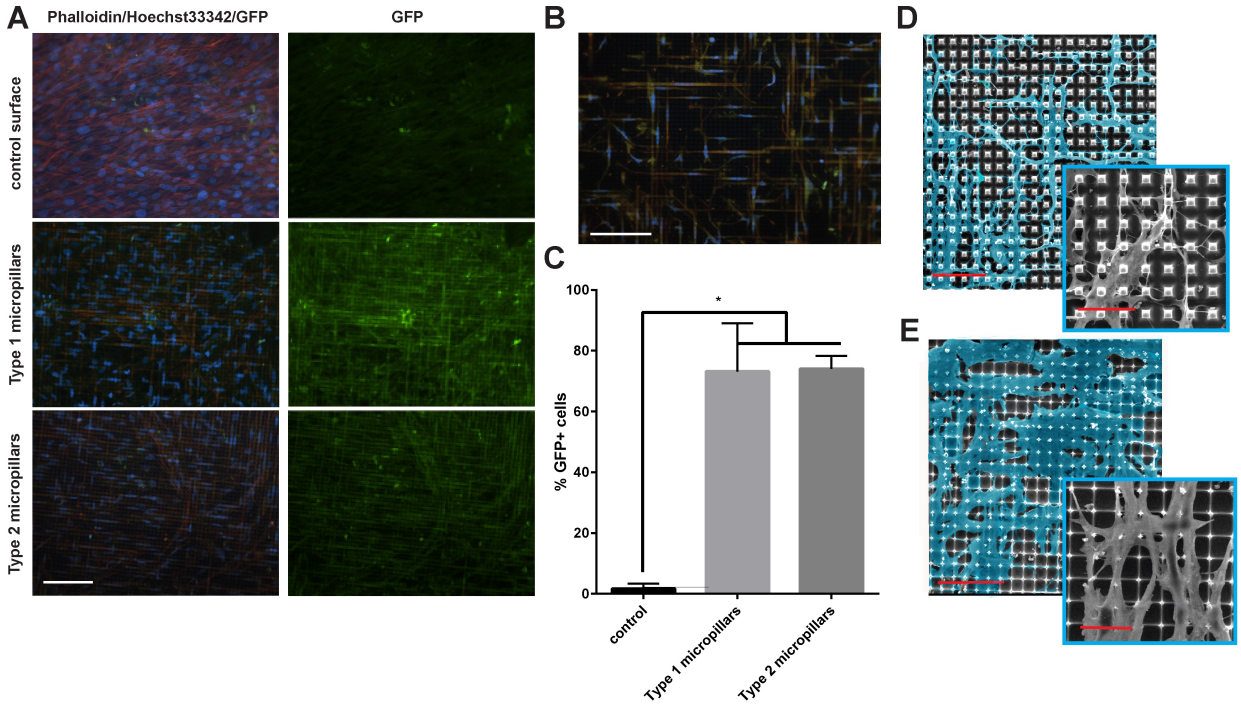

Figure 2. Human foreskin fibroblast (HFF) cells cultured on pillars exhibit a striking change in morphology. Associated with this, high levels of transfection occurred. Cells are stained with phalloidin to reveal the cytoskeleton (red) and Hoechst 33342 to reveal nuclei (blue). A) HFF transfection on flat silicon controls, type 1 and type 2 pillars. Scale bar 50 μm. B) Detail of transfected cells on type 1 pillars, stained with Hoechst 3342 (blue) and phalloidin (red) scale bar 50 μm. C) Quantification of HFF transfection on pillars (N≥ 3). D) Top view SEM images of HFF cultured on type 1 and E) type 2 pillars for 72 h. Scale bar = 50 μm. Inset scale bar 20μm.

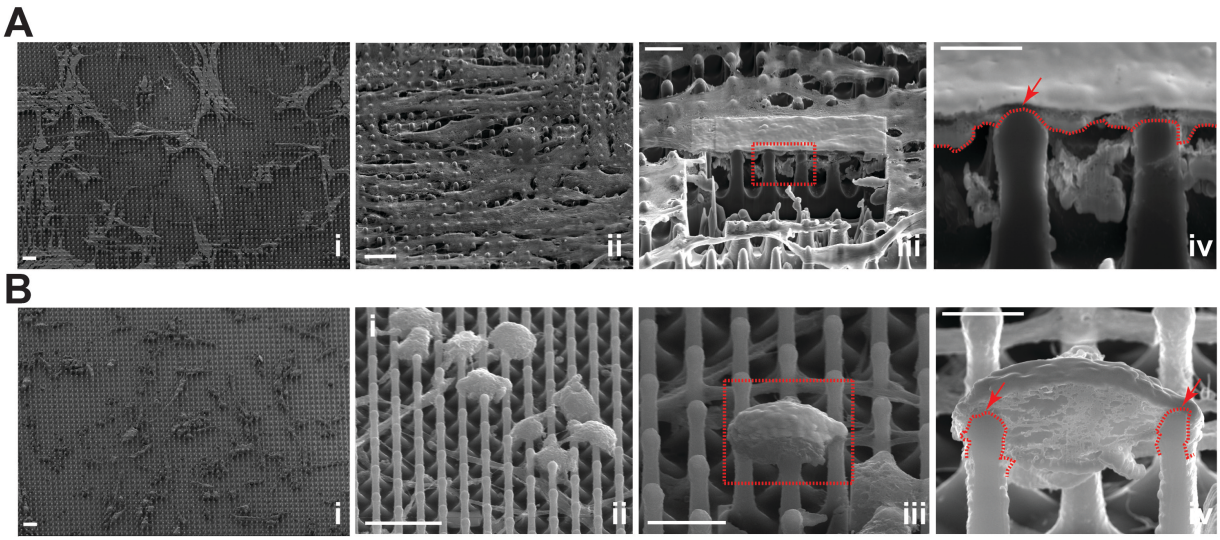

Figure 3. FIB-SEM analysis of HFF grown on type 1 pillars. i-ii)) overview of cell morphology, site of FIB-SEM analysis, iii) ion beam ablated site, red dotted line shows region displayed in panel iv; iv) tips of pillars penetrate into the cell. Red dotted line indicates interface between pillar structure and cell. Red arrows mark sites where pillars appear to extend through the cell membrane. A) and B) show HFF cells with representative morphology (A) extended, B) compact) observed on pillar substrates. Scale bars i-ii = 20 μm, iii = 10 μm; iv = 5 μm.

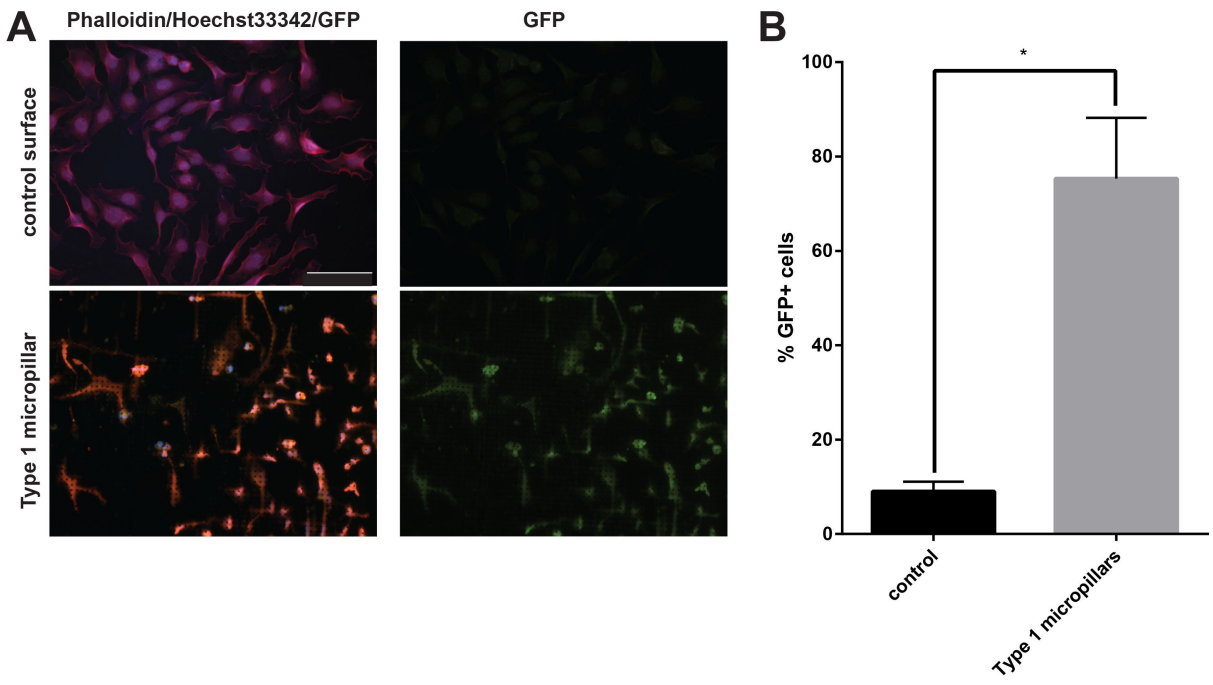

Figure 4. Transfection on pillar arrays is also high for other cell types. A) DPSC transfection on type 1 pillars and flat silicon substrates. Left: Cells were stained with phalloidin to reveal the cytoskeleton (red) and Hoechst 33342 to reveal nuclei (blue). Right: GFP expression in the corresponding cell population. Scale bar 50µm, B) Quantification of DPSC transfection on pillars (N≥ 3).

ASSOCIATED CONTENT

Supporting Information: protocols for fabrication of out-of-plane silicon micro pillar arrays, cell culture and transfection, examples of micro pillar topography tunability, images of viability and GFP expression control cultures, and additional FIB-SEM data sets. The Supporting Information is available free of charge via the Internet at http://pubs.acs.org.

AUTHOR INFORMATION

Corresponding Author

*E-mail: nico.voelcker@unisa.edu.au

*E-mail: g.barillaro@iet.unipi.it

Author Contributions

The manuscript was written through contributions of all authors. All authors have given approval to the final version of the manuscript. All the authors contributed equally.

ACKNOWLEDGMENT

This activity has been partially funded by the Italian Ministry of University and Research (MIUR) "Futuro in Ricerca" (FIR) programme, under the grant N. RBFR122KL1 (SENS4BIO).

REFERENCES

(1) Shalek, A. K.; Robinson, J. T.; Karp, E. S.; Lee, J. S.; Ahn, D.-R.; Yoon, M.-H.; Sutton, A.; Jorgolli, M.; Gertner, R. S.; Gujral, T. S.; Macbeath, G.; Yang, E. G.; Park, H. Vertical Silicon Nanowires as a Universal Platform for Delivering Biomolecules into Living Cells. *Proc. Natl. Acad. Sci. USA* **2010,** 107, 1870–1875.

(2) Bonde, S.; Buch-Manson, N.; Rostgaard, K. R.; Andersen, T. K.; Berthing, T.; Martinez, K. L. Exploring Arrays of Vertical One-Dimensional Nanostructures for Cellular Investigations. *Nanotechnology* **2014**, 25, 362001.

(3) Elnathan, R.; Kwiat, M.; Patolsky, F.; Voelcker, N. H. Engineering Vertically Aligned Semiconductor Nanowire Arrays for Applications in the Life Sciences. *Nano Today* **2014**, 9, 172–196.

(4) Prinz, C. N. Interactions Between Semiconductor Nanowires and Living Cells. *J. Phys.: Condens. Matter* **2015,** *27* (23), 233103

(5) Elnathan, R.; Delalat, B.; Brodoceanu, D.; Alhmoud, H.; Harding, F. J.; Buehler, K.; Nelson, A.; Isa, L.; Kraus, T.; Voelcker, N. H. Maximizing Transfection Efficiency of Vertically Aligned Silicon Nanowire Arrays. *Adv. Funct. Mater.* **2015**, 25, 7215-7225.

(6) Xie, X.; Xu, A. M.; Angle, M. R.; Tayebi, N.; Verma, P.; Melosh, N. A. Mechanical Model of Vertical Nanowire Cell Penetration. *Nano Lett.* **2013**, 13, 6002–6008.

(7) Xu, A. M.; Aalipour, A.; Leal-Ortiz, S.; Mekhdjian, A. H.; Xie, X.; Dunn, A. R.; Garner, C. C.; Melosh, N. A. Quantification of Nanowire Penetration Into Living Cells. *Nat. Commun.* **2014**, 5, 3613.

(8) Berthing, T.; Bonde, S.; Rostgaard, K. R.; Madsen, M. H.; Sorensen, C. B.; Nygard, J.; Martinez, K. L. Cell Membrane Conformation at Vertical Nanowire Array Interface Revealed by Fluorescence Imaging. *Nanotechnology* **2012**, 23, 415102.

(9) Hanson, L.; Lin, Z. C.; Xie, C.; Ciu, Y.; Ciu, B. Characterization Of the Cell–Nanopillar Interface by Transmission Electron Microscopy. *Nano Lett.* 2012, 12, 5815-5820

(10) Yosef, N.; Shalek, A. K.; Gaublomme, J. T.; Jin, H.; Lee, Y.; Awasthi, A.; Wu, C.; Karwacz, K.; Xiao, S.; Jorgolli, M.; Gennert, D.; Satija, R.; Shakya, A.; Lu, D. Y.;

Trombetta, J. J.; Pillai, M. R.; Ratcliffe, P. J.; Coleman, M. L.; Bix, M.; Tantin, D.; Park, H.; Kuchroo, V. K.; Regev, A., Dynamic Regulatory Network Controlling TH17 Cell Differentiation. *Nature* **2013**, 496, 461-468.

(11) Shalek, A. K.; Gaublomme, J. T.; Wang, L.; Yosef, N.; Chevrier, N.; Andersen, M. S.; Robinson, J. T.; Pochet, N.; Neuberg, D.; Gertner, R. S.; Amit, I.; Brown, J. R.; Hacohen, N.; Regev, A.; Wu, C. J.; Park, H. Nanowire-Mediated Delivery Enables Functional Interrogation of Primary Immune Cells: Application to the Analysis of Chronic Lymphocytic Leukemia. *Nano Lett*. **2012**, 12, 6498–6504.

(12) Kuo, S.-W.; Lin, H.-I.; Ho, J. H.-C.; Shih, Y.-R. V.; Chen, H.-F.; Yen, T.-J.; Lee, O. K. Regulation of the Fate of Human Mesenchymal Stem Cells by Mechanical and Stereo-Topographical Cues Provided by Silicon Nanowires. *Biomaterials* **2012**, 33, 5013–5022.

(13) Bonde, S.; Berthing, T.; Madsen, M. H.; Andersen, T. K.; Buch-Manson, N.; Guo, L.; Li, X.; Badique, F.; Anselme, K.; Nygård, J.; Martinez, K. L. Tuning Inas Nanowire Density for HEK293 Cell Viability, Adhesion, and Morphology: Perspectives for Nanowire-Based Biosensors. *ACS Appl. Mater. Interfaces*. **2013**, 5, 10510–10519.

(14) Bucaro, M. A.; Vasquez, Y.; Hatton, D. B.; Aizenberg, J. Fine-Tuning the Degree of Stem Cell Polarization and Alignment on Ordered Arrays of High-Aspect-Ratio Nano Pillars. *ACS Nano* **2012**, 6, 6222-6230

(15) Aalipour, A.; Xu, A. M.; Leal-Ortiz, S.; Garner, C. C.; Melosh, N. A. Plasma Membrane and Actin Cytoskeleton as Synergistic Barriers to Nanowire Cell Penetration. *Langmuir* **2014**, 30, 12362–12367.

(16) Bassu, M.; Surdo, S.; Strambini, L. M.; Barillaro, G. Electrochemical Micromachining as an Enabling Technology for Advanced Silicon Microstructuring. *Adv. Funct. Mater.* **2012**, 22, 1222-1228.

(17) S. Surdo, S. Merlo, F. Carpignano, L. M. Strambini, C. Trono, A. Giannetti, F. Baldini, G. Barillaro, Optofluidic microsystems with Integrated Vertical One-dimensional Photonic Crystals for Chemical Analysis, Lab Chip, **2012**, 12, 4403 - 4415.

(18) G. Barillaro, Silicon Electrochemical Micromachining Technology: the Good, the Bad, and the Future, *ECS Transactions,* **2015**, 69, 39-46.

(19) Dickinson, L. E.; Rand, D. R.; Tsao, J.; Eberle, W.; Gerecht, S. Endothelial Cell Responses to Micro pillar Substrates of Varying Dimensions and Stiffness. *J. Biomed. Mater. Res., Part A* **2012**, 100, 1457–1466.

(20) Gao, X.; Chau, Y. Y.; Xie, J.; Wan, J.; Ren, Y.; Qin, J.; Wen, W. Regulating Cell Behaviors on Micro pillar Topographies Affected by Interfacial Energy. *RSC Adv.* **2015**, 5, 22916–22922.

(21) Li, Z.; Song, J.; Mantini, G.; Lu, M.-Y.; Fang, H.; Falconi, C.; Chen, L. J.; Wang, Z. L. Quantifying the Traction Force of a Single Cell by Aligned Silicon Nanowire Array. *Nano Lett.* **2009**, 9, 3575–3580.

(22) Kim, D.-J.; Lee, G.; Kim, G.-S.; Lee, S.-K. Statistical Analysis Of Immuno-Functionalized Tumor-Cell Behaviors on Nanopatterned Substrates. *Nanoscale Res. Lett.* **2012**, 7, 637.

(23) Dalby, M. J.; Riehle, M. O.; Sutherland, D. S.; Agheli, H.; Curtis, A. S. G. Changes in Fibroblast Morphology in Response to Nano-Columns Produced by Colloidal Lithography. *Biomaterials* **2004**, 25, 5415–5422.

(24)Persson, H.; Li, Z.; Tegenfeldt, J. O.; Oredsson, S.; Prinz, C. N., From Immobilized Cells to Motile Cells on a Bed-of-nails: Effects of Vertical Nanowire Array Density on Cell behaviour. *Sci. Rep.* **2015**, 5, 18535.

(25) Wierzbicki, R.; Kobler, C.; Jensen, M. R. B.; Lopacinska, J.; Schmidt, M. S.; Skolimowski, M.; Abeille, F.; Qvortrup, K.; Molhave, K. Mapping the Complex Morphology of Cell Interactions with Nanowire Substrates using FIB-SEM. *Plos ONE* **2013**, 8, E53307.

(26) Kim, D.-J.; Seol, J.-K.; Lee, G.; Kim, G.-S.; Lee, S.-K. Cell Adhesion And Migration on Nanopatterned Substrates and their Effects on Cell-Capture Yield. *Nanotechnology* **2012**, 23, 395102.

(27) Tabaei, S. R.; Rabe, M.; Zhdanov, V. P.; Cho, N.-J.; Hook, F. Single Vesicle Analysis Reveals Nanoscale Membrane Curvature Selective Pore Formation in Lipid Membranes by an Antiviral Alpha-Helical Peptide. *Nano Lett.* **2012**, 12, 5719–5725.

(28) Bendix, P. M.; Pedersen, M. S.; Stamou, D. Quantification of Nano-Scale Intermembrane Contact Areas by Using Fluorescence Resonance Energy Transfer. *Proc. Natl. Acad. Sci. USA* **2009**, 106, 12341–12346.

(29) Buch-Månson, N.; Bonde, S.; Bolinsson, J.; Berthing, T.; Nygård, J.; Martinez, K. L. Towards a Better Prediction of Cell Settling on Nanostructure Arrays—Simple Means to Complicated Ends. *Adv. Funct. Mater.* **2015**, 25, 3246–3255.

(30) Cordella, N.; Lampo, T. J.; Melosh, N.; Spakowitz, A. J. Membrane Indentation Triggers Clathrin Lattice Reorganization and Fluidization. *Soft Matter* **2015**, 11, 439–448.

Table of Contents Graphic